



CM-P00056452

CERN-EP 90-80
c2

EUROPEAN ORGANIZATION FOR NUCLEAR RESEARCH

10 JUL. 1990

CERN-EP/90-80

8 June 1990

A Search for Sleptons and Gauginos in Z^0 Decays

DELPHI Collaboration

Abstract

Using a data sample corresponding to 10000 hadronic Z^0 decays, we have searched for the production of sleptons and gauginos in the two prong decays of Z^0 . No candidate remains after straightforward selections. For neutralinos, we use selection methods developed in our previous search for neutral Higgs particles. The negative results are translated into improved mass limits and parameter constraints on the minimal supersymmetric extension of the standard model.

(Submitted to Physics Letters B)

P.Abreu¹⁶, W.Adam³⁷, F.Adami²⁸, T.Adye²⁷, G.D.Alexeev¹², J.V.Allaby⁷, P.Allen³⁶, S.Almehed¹⁹,
 F.Alted³⁶, S.J.Alvsvaag⁴, U.Amaldi⁷, E.Anassontzis³, W-D.Apel¹³, B.Asman³², C.Astor Ferreres³⁰,
 J-E.Augustin¹⁵, A.Augustinus⁷, P.Baillon⁷, P.Bambade¹⁵, F.Barao¹⁶, G.Barbiellini³⁴, D.Y.Bardin¹²,
 A.Baroncelli²⁹, O.Barring¹⁹, W.Bartl³⁷, M.J.Bates²⁵, M.Baubillier¹⁸, K-H.Becks³⁹, C.J.Beeston²⁵,
 P.Beilliere⁶, I.Belokopytov³¹, P.Beltran⁹, D.Benedic⁸, J.M.Benloch³⁶, M.Berggren³², D.Bertrand²,
 S.Biagi¹⁷, F.Bianchi³³, J.H.Bibby²⁵, M.S.Bilenky¹², P.Billoir¹⁸, J.Bjarne¹⁹, D.Bloch⁸, P.N.Bogolubov¹²,
 D.Bollini⁵, T.Bolognese²⁸, M.Bonapart²², P.S.L.Booth¹⁷, M.Boratav¹⁸, P.Borgeaud²⁸, H.Borner²⁵,
 C.Bosio²⁹, O.Botner³⁵, B.Bouquet¹⁵, M.Bozzo¹⁰, S.Braibant⁷, P.Branchini²⁹, K.D.Brand³⁹,
 R.A.Brenner¹¹, C.Bricman², R.C.A.Brown⁷, N.Brummer²², J-M.Brunet⁶, L.Bugge²⁴, T.Buran²⁴,
 H.Burmeister⁷, C.Buttar²⁵, J.A.M.A.Buytaert², M.Caccia²⁰, M.Calvi²⁰, A.J.Camacho Rozas³⁰,
 J-E.Campagne⁷, A.Campion¹⁷, T.Camporesi⁷, V.Canale²⁹, F.Cao², L.Carroll¹⁷, C.Caso¹⁰, E.Castelli³⁴,
 M.V.Castillo Gimenez³⁶, A.Cattai⁷, F.R.Cavallo⁵, L.Cerrito²⁹, P.Charpentier⁷, P.Checchia²⁶,
 G.A.Chelkov¹², L.Chevalier²⁸, P.Chliapnikov³¹, V.Chorowicz¹⁸, R.Cirio³³, M.P.Clara³³,
 J.L.Contreras³⁶, R.Contri¹⁰, G.Cosme¹⁵, F.Couchot¹⁵, H.B.Crawley¹, D.Crennell²⁷, M.Cresti²⁶,
 G.Crosetti¹⁰, N.Crosland²⁵, M.Crozon⁶, J.Cuevas Maestro³⁰, S.Czellar¹¹, S.Dagoret¹⁵,
 E.Dahl-Jensen²¹, B.Dalmagne¹⁵, M.Dam⁷, G.Damgaard²¹, G.Darbo¹⁰, E.Daubie², M.Davenport⁷,
 P.David¹⁸, A.De Angelis³⁴, M.De Beer²⁸, H.De Boeck², W.De Boer¹³, C.De Clercq²,
 M.D.M.De Fez Laso³⁶, N.De Groot²², C.De La Vaissiere¹⁸, B.De Lotto³⁴, A.De Min²⁰, C.Defoix⁶,
 D.Delikaris⁷, P.Delpierre⁶, N.Demaria³³, L.Di Ciaccio²⁹, A.N.Diddens²², H.Dijkstra⁷, F.Djama⁸,
 J.Dolbeau⁶, K.Doroba³⁸, M.Dracos⁸, J.Drees³⁹, M.Dris²³, W.Dulinski⁸, R.Dzhelyadin³¹,
 D.N.Edwards¹⁷, L-O.Eek³⁵, P.A.-M.Eerola¹¹, T.Ekelof³⁵, G.Ekspong³², J-P.Engel⁸, V.Falaleev³¹,
 A.Fenyuk³¹, M.Fernandez Alonso³⁰, A.Ferrer³⁶, S.Ferroni¹⁰, T.A.Filippas²³, A.Firestone¹, H.Foeth⁷,
 E.Fokitis²³, F.Fontanelli¹⁰, H.Forsbach³⁹, B.Franek²⁷, K.E.Fransson³⁵, P.Frenkiel⁶, D.C.Fries¹³,
 R.Fruhwrith³⁷, F.Fulda-Quenzer¹⁵, H.Furstenau¹³, J.Fuster⁷, J.M.Gago¹⁶, G.Galeazzi²⁶, D.Gamba³³,
 U.Gasparini²⁶, P.Gavillet⁷, S.Gawne¹⁷, E.N.Gazis²³, P.Giacomelli⁵, K-W.Glitza³⁹, R.Gokieli¹⁸,
 V.M.Golovatyuk¹², A.Goobar³², G.Gopal²⁷, M.Gorski³⁸, Y.Gouz³¹, V.Gracco¹⁰, A.Grant⁷, F.Grard²,
 E.Graziani²⁹, I.A.Gritsaenko³¹, M-H.Gros¹⁵, G.Grosdidier¹⁵, B.Grossetete¹⁸, S.Gumenyuk³¹, J.Guy²⁷,
 F.Hahn³⁹, M.Hahn¹³, S.Haider⁷, Z.Hajduk²², A.Hakansson¹⁹, A.Hallgren³⁵, K.Hamacher³⁹,
 G.Hamel De Monchenault²⁸, F.J.Harris²⁵, B.Heck⁷, I.Herbst³⁹, J.J.Hernandez³⁶, P.Herquet², H.Herr⁷,
 E.Higon³⁶, H.J.Hilke⁷, T.Hofmoki³⁸, R.Holmes¹, S-O.Holmgren³², J.E.Hooper²¹, M.Houlden¹⁷,
 J.Hrubic³⁷, P.O.Hulth³², K.Hultqvist³², D.Husson⁸, B.D.Hyams⁷, P.Ioannou³, P-S.Iversen⁴,
 J.N.Jackson¹⁷, P.Jalocha¹⁴, G.Jarlskog¹⁹, P.Jarry²⁸, B.Jean-Marie¹⁵, E.K.Johansson³², M.Jonker⁷,
 L.Jonsson¹⁹, P.Juillot⁸, R.B.Kadyrov¹², G.Kalkanis³, G.Kalmus²⁷, G.Kantardjian⁷, F.Kapusta¹⁸,
 P.Kapusta¹⁴, S.Katsanevas³, E.C.Katsoufis²³, R.Keranen¹¹, J.Kesteman², B.A.Khomenko¹², B.King¹⁷,
 N.J.Kjaer²¹, H.Klein⁷, W.Klempt⁷, A.Klovning⁴, P.Kluit², J.H.Koehne¹³, B.Koene²², P.Kokkinias⁹,
 M.Kopf¹³, M.Koratzinos⁷, K.Korcyll¹⁴, A.V.Korytov¹², B.Korzen⁷, C.Kourkoumelis³, T.Kreuzberger³⁷,
 J.Krolkowski³⁸, U.Kruener-Marquis³⁹, W.Krupinski¹⁴, W.Kucewicz²⁰, K.Kurvinen¹¹, M.I.Laakso¹¹,
 C.Lambropoulos⁹, J.W.Lamsa¹, L.Lanceri³⁴, V.Lapchine³¹, V.Lapin³¹, J-P.Laugier²⁸,
 R.Lauhakangas¹¹, P.Laurikainen¹¹, G.Leder³⁷, F.Ledroit⁶, J.Lemonne², G.Lenzen³⁹, V.Lepeltier¹⁵,
 A.Letessier-Selvon¹⁸, E.Lieb³⁹, E.Lillestol⁷, E.Lillethun⁴, J.Lindgren¹¹, I.Lippi²⁶, R.Llosa³⁶,
 B.Loerstad¹⁹, M.Lokajicek¹², J.G.Loken²⁵, M.A.Lopez Aguera³⁰, A.Lopez-Fernandez¹⁵, D.Loukas⁹,
 J.J.Lozano³⁶, R.Lucocock²⁷, B.Lund-Jensen³⁵, P.Lutz⁶, L.Lyons²⁵, G.Maehlum⁷, J.Maillard⁶,
 A.Maltesos⁹, F.Mandl³⁷, J.Marco³⁰, J-C.Marin⁷, A.Markou⁹, L.Mathis⁶, C.Matteuzzi²⁰, G.Matthiae²⁹,
 M.Mazzucato²⁶, M.Mc Cubbin¹⁷, R.Mc Kay¹, E.Menichetti³³, C.Meroni²⁰, W.T.Meyer¹,
 W.A.Mitaroff³⁷, G.V.Mitselmakher¹², U.Mjoernmark¹⁹, T.Moa³², R.Moeller²¹, K.Moenig³⁹,
 M.R.Monge¹⁰, P.Morettini¹⁰, H.Mueller¹³, H.Muller⁷, G.Myatt²⁵, F.Naraghi¹⁸, U.Nau-Korzen³⁹,
 F.L.Navarria⁵, P.Negri²⁰, B.S.Nielsen²¹, M.Nigro²⁶, V.Nikolaenko³¹, V.Obrastsov³¹, R.Orava¹¹,
 A.Ouraou²⁸, R.Pain¹⁸, H.Palka¹⁴, T.Papadopoulou²³, L.Pape⁷, P.Pasini⁵, A.Passeri²⁹, M.Pegoraro²⁶,
 V.Perevozchikov³¹, M.Pernicka³⁷, M.Pimenta¹⁶, O.Pingot², C.Pinori²⁶, A.Pinsent²⁵, M.E.Pol¹⁶,
 G.Polok¹⁴, P.Poropat³⁴, P.Privitera⁵, A.Pullia²⁰, J.Pyyhtia¹¹, A.A.Rademakers²², D.Radojicic²⁵,
 S.Ragazzi²⁰, W.H.Range¹⁷, P.N.Ratoff²⁵, A.L.Read²⁴, N.G.Redaeli²⁰, M.Regler³⁷, D.Reid¹⁷,
 P.B.Renton²⁵, L.K.Resvanis³, F.Richard¹⁵, J.Ridky¹², G.Rinaudo³³, I.Roditi⁷, A.Romero³³,
 P.Ronchese²⁶, E.I.Rosenberg¹, U.Rossi⁵, E.Rosso⁷, P.Roudeau¹⁵, T.Rovelli⁵, V.Ruhlmann²⁸, A.Ruiz³⁰,
 H.Saarikko¹¹, Y.Sacquin²⁸, E.Sanchez³⁶, J.Sanchez³⁶, E.Sanchis³⁶, M.Sannino¹⁰, M.Schaeffer⁸,
 H.Schneider¹³, F.Scuri³⁴, A.Sebastia³⁶, A.M.Segar²⁵, R.Sekulin²⁷, M.Sessa³⁴, G.Sette¹⁰, R.Seufert¹³,
 R.C.Shellard⁷, P.Siegrist²⁸, S.Simonetti¹⁰, F.Simonetto²⁶, A.N.Sissakian¹², T.B.Skaali²⁴, J.Skeens¹,
 G.Skjevling²⁴, G.Smadja²⁸, G.R.Smith²⁷, R.Sosnowski³⁸, K.Spang²¹, T.Spassoff¹², E.Spiriti²⁹,
 S.Squarcia¹⁰, H.Staek³⁹, C.Stanescu²⁹, G.Stavropoulos⁹, F.Stichelbaut², A.Stocchi²⁰, J.Strauss³⁷,

R.Strub⁸, C.J.Stubenrauch⁷, M.Szczekowski³⁸, M.Szeptycka³⁸, P.Szymanski³⁸, S.Tavernier², G.Theodosiou⁹, A.Tilquin⁶, J.Timmermans²², V.G.Timofeev¹², L.G.Tkatchev¹², D.Z.Toet²², A.K.Toppol⁴, L.Tortora²⁹, D.Treille⁷, U.Trevisan¹⁰, G.Tristram⁶, C.Troncon²⁰, E.N.Tsyganov¹², M.Turala¹⁴, R.Turchetta⁸, M-L.Turluer²⁸, T.Tuuva¹¹, I.A.Tyapkin¹², M.Tyndel²⁷, S.Tzamarias⁷, F.Udo²², S.Ueberschaer³⁹, V.A.Uvarov³¹, G.Valenti⁵, E.Vallazza³³, J.A.Valls Ferrer³⁶, G.W.Van Apeldoorn²², P.Van Dam²², W.K.Van Doninck², N.Van Eijndhoven⁷, C.Vander Velde², J.Varela¹⁶, P.Vaz¹⁶, G.Vegni²⁰, M.E.Veitch²⁵, J.Velasco³⁶, L.Ventura²⁶, W.Venus²⁷, F.Verbeure², L.S.Vertogradov¹², L.Vibert¹⁸, D.Vilanova²⁸, E.V.Vlasov³¹, A.S.Vodopyanov¹², M.Vollmer³⁹, G.Voulgaris³, M.Voutilainen¹¹, V.Vrba¹², H.Wahlen³⁹, C.Walck³², F.Waldner³⁴, M.Wayne¹, P.Weilhammer⁷, J.Werner³⁹, A.M.Wetherell⁷, J.H.Wickens², J.Wikne²⁴, W.S.C.Williams²⁵, M.Winter⁸, D.Wormald²⁴, G.Wormser¹⁵, K.Woschnagg³⁵, N.Yamdagni³², P.Yepes²², A.Zaitsev³¹, A.Zalewska¹⁴, P.Zalewski³⁸, P.I.Zarubin¹², E.Zevgolatakos⁹, G.Zhang³⁹, N.I.Zimin¹², R.Zitoun¹⁸, R.Zukanovich Funchal⁶, G.Zumerle²⁶, J.Zuniga³⁶

-
- ¹Ames Laboratory and Department of Physics, Iowa State University, Ames IA 50011, USA
²Physics Department, Univ. Instelling Antwerpen, Universiteitsplein 1, B-2610 Wilrijk, Belgium and IIHE, ULB-VUB, Pleinlaan 2, B-1050 Brussels, Belgium
and Service de Phys. des Part. Elém., Faculté des Sciences, Université de l'Etat Mons, Av. Maistriau 19, B-7000 Mons, Belgium
³Physics Laboratory, University of Athens, Solonos Str. 104, GR-10680 Athens, Greece
⁴Department of Physics, University of Bergen, Allégaten 55, N-5007 Bergen, Norway
⁵Dipartimento di Fisica, Università di Bologna and INFN, Via Irnerio 46, I-40126 Bologna, Italy
⁶Collège de France, Lab. de Physique Corpusculaire, 11 pl. M. Berthelot, F-75231 Paris Cedex 05, France
⁷CERN, CH-1211 Geneva 23, Switzerland
⁸Division des Hautes Energies, CRN - Groupe DELPHI, B.P. 20 CRO, F-67037 Strasbourg Cedex, France
⁹Greek Atomic Energy Commission, Nucl. Research Centre Demokritos, P.O. Box 60228, GR-15310 Aghia Paraskevi, Greece
¹⁰Dipartimento di Fisica, Università di Genova and INFN, Via Dodecaneso 33, I-16146 Genova, Italy
¹¹Dept. of High Energy Physics, University of Helsinki, Siltavuorenpenger 20 C, SF-00170 Helsinki 17, Finland
¹²Joint Institute for Nuclear Research, Dubna, Head Post Office, P.O. Box 79, 101 000 Moscow, USSR.
¹³Institut für Experimentelle Kernphysik, Universität Karlsruhe, Postfach 6980, D-7500 Karlsruhe 1, FRG
¹⁴High Energy Physics Laboratory, Institute of Nuclear Physics, Ul. Kawioro 26 a, PL-30055 Krakow 30, Poland
¹⁵Université de Paris-Sud, Lab. de l'Accélérateur Linéaire, Bat 200, F-91405 Orsay, France
¹⁶LIP, Av. Elias Garcia 14 - 1e, P-1000 Lisbon Codex, Portugal
¹⁷Department of Physics, University of Liverpool, P.O. Box 147, GB - Liverpool L69 3BX, UK
¹⁸LPNHE, Universités Paris VI et VII, Tour 33 (RdC), 4 place Jussieu, F-75230 Paris Cedex 05, France
¹⁹Department of Physics, University of Lund, Sölvegatan 14, S-22363 Lund, Sweden
²⁰Dipartimento di Fisica, Università di Milano and INFN, Via Celoria 16, I-20133 Milan, Italy
²¹Niels Bohr Institute, Blegdamsvej 17, DK-2100 Copenhagen 0, Denmark
²²NIKHEF-H, Postbus 41882, NL-1009 DB Amsterdam, The Netherlands
²³National Technical University, Physics Department, Zografou Campus, GR-15773 Athens, Greece
²⁴Physics Department, University of Oslo, Blindern, N-1000 Oslo 3, Norway
²⁵Nuclear Physics Laboratory, University of Oxford, Keble Road, GB - Oxford OX1 3RH, UK
²⁶Dipartimento di Fisica, Università di Padova and INFN, Via Marzolo 8, I-35131 Padua, Italy
²⁷Rutherford Appleton Laboratory, Chilton, GB - Didcot OX11 0QX, UK
²⁸CEN-Saclay, DPhPE, F-91191 Gif-sur-Yvette Cedex, France
²⁹Istituto Superiore di Sanità, Ist. Naz. di Fisica Nucl. (INFN), Viale Regina Elena 299, I-00161 Rome, Italy and Dipartimento di Fisica, Università di Roma II and INFN, Tor Vergata, I-00173 Rome.
³⁰Facultad de Ciencias, Universidad de Santander, av. de los Castros, E - 39005 Santander, Spain
³¹Inst. for High Energy Physics, Serpukov P.O. Box 35, Protvino, (Moscow Region), USSR.
³²Institute of Physics, University of Stockholm, Vanadisvägen 9, S-113 46 Stockholm, Sweden
³³Dipartimento di Fisica Sperimentale, Università di Torino and INFN, Via P. Giuria 1, I-10125 Turin, Italy
³⁴Dipartimento di Fisica, Università di Trieste and INFN, Via A. Valerio 2, I-34127 Trieste, Italy and Istituto di Fisica, Università di Udine, I-33100 Udine, Italy
³⁵Department of Radiation Sciences, University of Uppsala, P.O. Box 535, S-751 21 Uppsala, Sweden
³⁶Inst. de Fisica Corpuscular IFIC, Centro Mixto Univ. de Valencia-CSIC, Avda. Dr. Moliner 50, E-46100 Burjassot (Valencia), Spain
³⁷Institut für Hochenergiephysik, Österreich Akad. d. Wissensch., Nikolsdorfergasse 18, A-1050 Vienna, Austria
³⁸Inst. Nuclear Studies and, University of Warsaw, Ul. Hoza 69, PL-00681 Warsaw, Poland
³⁹Fachbereich Physik, University of Wuppertal, Postfach 100 127, D-5600 Wuppertal 1, FRG

INTRODUCTION

This paper presents a systematic search for heavy supersymmetric partners of charged leptons, gauge bosons and Higgs particles. The data have been collected during the energy scan of the Z^0 performed at LEP at the end of 1989. In this introduction, we review the supersymmetry concepts relevant to our analysis and outline our selection methods to eliminate the background.

In the supersymmetric scheme[1], one expects two charged and three neutral Higgs particles. Accordingly there should be four neutralinos, the spin 1/2 mass eigenstates formed by mixing the weak eigenstates associated to Z^0 and γ and to the neutral Higgs scalars. Similarly, there are two pairs of charginos formed by mixing the weak eigenstates associated to W bosons (winos) and to charged Higgs particles (higgsinos). The lightest chargino pair is called χ^\pm , and χ , χ' and χ'' are the three lightest neutralinos ordered by mass. In the minimal supersymmetric extension of the standard model, the so-called MSSM scheme[1], all relevant physical quantities, masses and mixing angles of charginos and neutralinos, can be expressed in terms of two mass parameters, μ and M, and of the angle β , $\tan\beta$ being the ratio of vacuum expectations generated in the two Higgs doublet model. In particular, this model predicts a sizeable coupling of Z^0 into $\chi\chi'$, $\chi'\chi'$ and even $\chi\chi''$ states. The coupling of Z^0 into $\chi^+\chi^-$ is predicted to be large for all masses accessible to Z^0 decays.

In this model, there are two heavy scalar particles, called sleptons, associated with the standard chiral leptonic states which are denoted $\tilde{\ell}_R^\pm$ and $\tilde{\ell}_L^\pm$. $\tilde{\ell}_R$ is expected to be the lightest but we will also test the case of degenerate masses.

In the simplest scenario, χ is the lightest supersymmetric particle and one foresees the following decays :

$$\chi^\pm \rightarrow \chi W^{*\pm} \text{ with } W^{*\pm} \rightarrow \ell^\pm \nu$$

$$\tilde{\ell}^\pm \rightarrow \chi \ell^\pm$$

$$\chi' \rightarrow \chi Z^* \text{ with } Z^* \rightarrow \ell^+ \ell^-$$

The latter decay is dominant when the neutral Higgs boson is heavier than 10 GeV/c². The lightest neutralino, χ , is assumed to be stable and to go undetected since it has only weak interactions.

The Z^0 decays into heavy sleptons, chargino and neutralino states can give acollinear two prong events with large missing energy. To improve the efficiency for the neutralino channel, we have also considered the hadronic decays of the virtual Z which give final states very similar to the $q\bar{q}\nu\bar{\nu}$ and $q\bar{q}\ell^+\ell^-$ channels previously studied in our Higgs search[2,3].

If the lightest supersymmetric particle is not neutral, one could observe Z^0 's decaying into two heavy stable charged particles. The final state is identified kinematically by looking for elastic two prongs with a measured momentum which differs significantly from the beam momentum :

$$\delta p = p_{beam} - p \simeq m_{\tilde{\ell}}^2/2p$$

With a magnetic field of 1.23 Tesla, the momentum measurement error in DELPHI is $\Delta p/p^2 = 2.10^{-3} (\text{GeV}/c)^{-1}$ which allows us to set limits for $m_{\tilde{\ell}} > 25\text{GeV}/c^2$.

After specifying in section 1 the production cross sections used and describing the apparatus in section 2, the details of event selection are given in section 3. In section 4 the corresponding efficiencies are given and the results are presented in section 5 for sleptons, charginos and neutralinos - as well as the limits obtained on the minimal supersymmetric standard model (MSSM) parameters.

1 CROSS SECTIONS, ANGULAR DISTRIBUTIONS

i) Sleptons

The cross section for the production of slepton pairs of mass $m_{\tilde{\ell}}$ is :

$$\sigma_{\tilde{\ell}_R^+\tilde{\ell}_R^-} \simeq \sigma_{\tilde{\ell}_L^+\tilde{\ell}_L^-} \simeq \frac{\beta_{\tilde{\ell}}^3}{8} \sigma_{\nu\bar{\nu}} \quad \text{where } \beta_{\tilde{\ell}} = \sqrt{1 - \frac{4m_{\tilde{\ell}}^2}{m_{Z^0}^2}}$$

$\sigma_{\nu\bar{\nu}}$ is the resonant neutrino pair production cross section, and m_{Z^0} is the Z^0 mass.

The distribution of the polar angle of the outgoing $\tilde{\ell}^-$ with respect to the e^- incoming direction is proportional to $\sin^2\theta$. The scalar $\tilde{\ell}$ decays into its partner lepton and a χ with an isotropic angular distribution.

ii) Charginos

For charginos, the vector and axial couplings depend on two mixing angles ϕ_+ and ϕ_- :

$$C_V = -\frac{\cos^2 \phi_+ + \cos^2 \phi_-}{4} - \frac{1}{2} + \sin^2 \theta_w$$

$$C_A = \frac{\cos^2 \phi_+ - \cos^2 \phi_-}{4}$$

and the cross-section is:

$$\sigma_{\chi^+\chi^-} = 8\beta_\chi \left[C_V^2 \frac{3 - \beta_\chi^2}{2} + C_A^2 \beta_\chi^2 \right] \sigma_{\nu\bar{\nu}} \quad \text{where } \beta_\chi = \sqrt{1 - \frac{4m_\chi^2}{m_Z^2}}$$

m_χ is the chargino mass, and θ_w is the weak mixing angle.

$\phi_+ = \phi_- = 0$ corresponds to the production of a pure wino while the minimal cross section is reached for the pure higgsino case $\phi_+ = \phi_- = \frac{\pi}{2}$:

$$\sigma_{\chi^+\chi^-}^{\min} = \cos^2(2\theta_W) \beta_\chi (3 - \beta_\chi^2) \sigma_{\nu\bar{\nu}}$$

In both cases, the axial term is zero and the angular distribution of χ^- with respect to the e^- incoming direction is given by :

$$\frac{d\sigma}{d\cos\theta} \sim 1 + \cos^2\theta + (1 - \beta_\chi^2) \sin^2\theta$$

iii) Neutralinos

The decay rates of Z^0 to $\chi\chi'$, $\chi'\chi'$ and $\chi\chi''$ are essentially unknown since they not only depend on the masses of the two neutralinos but also on their composition in terms of the gaugino and higgsino fields. In the favourable cases for which the higgsino component dominates, $\Gamma(Z \rightarrow \chi\chi')$ can be very large, of the order of the width $\Gamma(Z \rightarrow \nu\bar{\nu})$, thus allowing a meaningful search in the two prong channel.

The angular distribution of the final state fermions is fairly complicated. Following ref. [1], we have ignored the correlations due to the spin of the decaying χ' and used the simplified matrix element given in [1]. This approximation has a negligible effect on the computed acceptance.

We assume that χ' and χ'' dominantly decay into $\chi f\bar{f}$ through a virtual Z^0 , as is true in the MSSM scheme except, possibly, for particular values of the (μ, M) parameters for which the process $\chi' \rightarrow \chi\gamma$ can contribute substantially [4].

2 APPARATUS

A detailed description of the DELPHI detector, of the triggering conditions and of the analysis chain can be found in [5]. Here, only the specific properties relevant to the following analysis are summarized.

The charged tracks are measured in the 1.23 Tesla magnetic field by a set of three cylindrical tracking detectors : the inner Detector (ID) covers radii 12 to 28 cm, the Time Projection Chamber (TPC) from 30 to 122 cm, and the Outer Detector (OD) between 198 and 206 cm. The end caps are covered by the Forward Chambers A and B, at polar angles 10° to 36° on each side. A layer of Time-of-Flight (TOF) counters is installed for triggering purposes beyond the magnet coil.

The electromagnetic energy is measured in the High Density Projection Chamber (HPC), and by the Forward Electromagnetic Calorimeter (FEMC) in the end caps. The HPC is a high granularity gaseous calorimeter covering polar angles 40° to 140° . For fast triggering a scintillation layer is installed after the first 5 radiation lengths of lead. The FEMC consists of 2×4500 lead glass blocks (granularity 1×1 degrees), covering polar angles from 10° to 36° on each side.

The trigger is based on the ID and OD coincidences, on the HPC and TOF scintillation counters, and on the forward detectors. The track trigger is formed using opposite quadrants of the OD in coincidence with the ID trigger layer. The counter trigger uses half length quadrants of TOF counters sensitive to penetrating charged particles, and HPC counters sensitive to electromagnetic showers with an energy greater than 2 GeV, arranged in various sets of back-to-back and majority logics. The forward trigger is made from the same side coincidences of Chambers A and B , combined with the two FEMC signals in a majority logic. The efficiency of these various triggers is measured with the Z^0 data, by analyzing the recorded trigger patterns, and is applied to the simulated data.

The present analysis relies primarily on charged tracks reconstructed using the TPC, complemented by the Inner and the Outer detectors. In some small azimuthal regions which correspond to six boundaries of the TPC sectors, this efficiency drops for energetic ($p > 4$ GeV/c) tracks. The electromagnetic calorimetry is used to veto against photons emitted at large angle in standard decays of the Z^0 to lepton pairs.

3 EVENT SELECTION

i) Two prongs

In order to accommodate the possibility of a heavy χ , one should choose the momentum cut on the two prong final states at the smallest possible level compatible with the backgrounds coming from $Z \rightarrow \tau^+ \tau^-$ and $\gamma \gamma \rightarrow \ell^+ \ell^-$. The $\gamma \gamma$ process[6], relatively unimportant at the Z^0 resonance, naturally peaks at low acoplanarity (acollinearity in the plane transverse to the beam) and tends to give tracks with low transverse momenta. It is reduced to a few picobarns with a cut on acoplanarity at 15° , and by demanding at least one charged particle with a transverse momentum above 1.5 GeV/c and both charged particles at more than 25° with respect to the beam axis. The $\tau^+ \tau^-$ background[7], as shown in Fig.1, also peaks at low acoplanarity provided momenta above 2 GeV/c are selected. We thus require events with two oppositely charged tracks which fulfill these cuts. These two tracks are also required to form a vertex falling inside a 2 cm radius and 10 cm long cylinder around the beam position. To avoid any contamination from final state radiation with an undetected photon, the analysis for the two prong channel is restricted to a sample corresponding to 6000 hadronic Z^0 , for which the electromagnetic calorimeters were fully operational.

After these selections, two events remain. Both have an energetic photon coplanar with the two charged tracks and at more than 30° from each of them. The Monte Carlo based on the standard leptonic generators[7] predicts 3.0 ± 0.8 events with such a large angle photon. These two events are thus rejected as due to standard lepton pair production with final state radiation.

ii) Stable charged particles

For stable charged particle searches we look for muon-like candidates with accurately measured momenta. We therefore reject one third of the data which were recorded at reduced magnetic field and select events at $|\cos \theta| \leq 0.65$ in which both tracks are measured by TPC and OD. We require that no shower be present in the HPC, which removes nearly all $e^+ e^-$ and a large fraction of $\tau^+ \tau^-$ final states. Finally we retain only events for which both momenta are larger than 10 GeV/c. Most of the remaining $\tau^+ \tau^-$ are eliminated by asking for an acollinearity angle below 15 mrad and an acoplanarity angle below 10 mrad. Figure 2 shows the correlations between p^+ and p^- , the

measured momenta of the two prong candidates retained by these selections. A pair of heavy charged particles would fall on the diagonal, below the beam momentum region which is populated by standard muon pairs.

The observed distribution shows no clustering outside the beam momentum region. In figure 2 are shown two $1-\sigma$ contours that would correspond to stable particles with masses of $25 \text{ GeV}/c^2$ and $40 \text{ GeV}/c^2$. The spread in measured momenta allows us to set limits above $25 \text{ GeV}/c^2$ in a mass range not covered by TRISTAN[8] and PETRA[9]. For a $\tilde{\ell}_R$ with a mass of $25 \text{ GeV}/c^2$ one expects 15 events of which 6 are clustered inside the corresponding contour.

iii) Neutralinos with hadronic decays

The three following channels have been considered:

$$Z \rightarrow \chi\chi'(\text{or}\chi'') \rightarrow q\bar{q}\chi\chi \quad (\text{a})$$

$$Z \rightarrow \chi'\chi' \rightarrow q\bar{q}\nu\bar{\nu}\chi\chi \quad (\text{b})$$

$$Z \rightarrow \chi'\chi' \rightarrow q\bar{q}\ell^+\ell^-\chi\chi \quad (\text{c})$$

A search for Z^0 to $H^0\nu\bar{\nu}$ with topologies similar to (a) and (b) was reported in ref. [2]. The sample corresponded to 10950 hadronic events and no candidate was found provided one rejected events with a total mass of charged particles above $40 \text{ GeV}/c^2$. As shown below, the corresponding selection criteria give a reasonable efficiency for channels (a) and (b) for the relevant μ and M parameters.

Channel (c), which gives 2 isolated leptons with jets, is analyzed as in ref. [3] where we conclude that our data do not contain any event consistent with such a topology.

4 EFFICIENCIES

i) Two prong final states

The acceptance of the track trigger for two charged particles, which imposes a loose back-to-back topology, is above 50% for the $\tilde{\ell}^+\tilde{\ell}^-$ channel for $m_{\tilde{\ell}} < 25 \text{ GeV}/c^2$. For charginos and heavy sleptons, we rely mostly on the counter trigger which can be satisfied when two showers of more than 2 GeV appear in the HPC or when one shower is in coincidence with the TOF counters. This condition is well fulfilled not only for ee

or μe final states but also for $e\tau$, $\tau\tau$ and $\mu\tau$ final states since more than half of the τ decays provide electromagnetic energy.

The result is that, with the exception of $\tilde{\mu}^+\tilde{\mu}^-$, the global trigger efficiency for two prongs is above 40 %.

Tables 1 and 2 summarize the efficiencies for the various channels taking into account triggering and the various selections described in the previous section. Due to the mildness of the cuts used in this analysis, the efficiencies vary only slowly with the neutralino masses.

ii) Hadronic final states

For channels (a) and (b), the trigger efficiency is above 50% in the relevant (μ, M) domain. Table 3 gives a sample of efficiencies relevant to the neutralino search. The efficiency drops for heavy χ' (or χ'') since the selections have been optimized for $H^0\nu\bar{\nu}$ assuming a light neutral Higgs.

5 RESULTS

Sleptons

With no candidate for supersymmetric channels, we can derive limits in terms of $m_{\tilde{l}}$ and m_{χ} with two assumption :

$$m_{\tilde{l}_R} = m_{\tilde{l}_L} \quad \text{or} \quad m_{\tilde{l}_L} \gg m_{\tilde{l}_R}$$

Figure 3 shows the limits corresponding to the three lepton families. These limits reach 40 GeV/c² for selectrons and all limits greatly improve the results from PEP[10] and TRISTAN[8]. At lower $m_{\tilde{l}}$ masses, a remarkable improvement comes from the absence of $\gamma\gamma$ background at the Z^0 peak, which makes accessible the region where $m_{\tilde{l}} \sim m_{\chi}$. This effect is even more critical for the $\tilde{\tau}$ limits. Similar limits have been obtained by other LEP experiments[11].

The limits on stable $\tilde{\ell}^{\pm}$ are flavour independent: masses between 25 GeV/c² and 40 GeV/c² are excluded.

Charginos

Limits for the pure higgsino and pure gaugino cases are given in figure 4. They reach the kinematical limit as in ref. [11]. The selection based on leptons covers the region $m_{\chi^\pm} \sim m_\chi$, whereas an analysis based on hadronic decays may be more delicate to interpret.

The limit on stable χ^\pm reaches $45 \text{ GeV}/c^2$ and is complemented in the low mass region by the TRISTAN results[8].

Neutralinos

As pointed out in the introduction, the rate for neutralinos is very model dependent. The present analysis excludes $\text{BR}(Z \rightarrow \chi\chi') \geq 10^{-3}$ and $\text{BR}(Z \rightarrow \chi'\chi') \geq 2 \cdot 10^{-3}$ assuming that the χ' decays into $\chi f \bar{f}$ through a virtual Z^0 . These limits vary slowly with the masses of the neutralinos as shown in efficiency tables 2 and 3. Similar results were obtained in [12].

Limits on the MSSM parameters

In the MSSM scheme all quantities relevant to gauginos are fixed by μ , M and $\tan\beta$. We choose $\tan\beta = 2$ and $\tan\beta = 4$ and show in figure 5 the (μ, M) region rejected by our results. The region inside the hatched curves is excluded by the non-observation of neutralinos or charginos, with some complementarity as shown by the corresponding lines.

The dashed lines delimit a zone where theory predicts stable charginos with $m_{\chi^\pm} \leq 20 \text{ GeV}/c^2$, which have been excluded by the TRISTAN results (figure 4). Just outside the border lines, where charginos become unstable with m_{χ^\pm} close to m_χ , there is a narrow domain not excluded by our search for charginos (see figure 4), but partially excluded by our search for neutralinos.

The excluded region is extended significantly when $\tan\beta$ increases.

Given the large branching ratios for Z^0 decays into gauginos predicted by MSSM, one can already exclude a large (μ, M) domain using purely inclusive arguments based on the measured widths of the Z^0 . These limits are however ambiguous since, as pointed out in ref. [13], it is not easy to determine which gaugino channels contribute to the hadronic width and which correspond to the invisible part. Even if one ignores such

limitations, the domain which can be covered by the inclusive results is narrower than the one covered by the present analysis.

CONCLUSIONS

Using various selection methods based on acoplanar lepton events and hadronic events with isolated leptons or with large missing energy, we have searched for the presence of heavy sleptons and gauginos for a wide range of masses. Since no candidate was found, we are able to set limits on the Z^0 branching ratios to such objects at the level of 10^{-3} . These limits severely constrain the parameters of the MSSM model.

Acknowledgements

This study has benefited from numerous discussions with G.Ridolfi.

We are greatly indebted to our technical staff and collaborators and funding agencies for their support in building the DELPHI detector, and to the members of the LEP Division for the speedy commissioning and superb performance of the LEP collider.

References

- [1] R.Barbieri et al., Z^0 Physics at LEP 1, Supersymmetry searches, CERN 89-08, vol.2, p.121 and references therein.
- [2] DELPHI collaboration, P.Abreu et al., CERN/EP 90-44, to be published in Nucl. Phys. B.
- [3] DELPHI Collaboration, Search for Pair Production of Neutral Higgs Bosons in Z^0 Decays (in preparation).
- [4] R.Barbieri, G.Gamberini, G.F.Giudice and G. Ridolfi, Nucl. Phys. B296 (1988) 75;
H.E.Haber and D.Wyler, Nucl. Phys. B323 (1989) 267.
- [5] DELPHI collaboration, P.Aarnio et al., Phys. Lett. B231 (1989) 539;
The Delphi Detector(to be published).
- [6] F.A.Berends and P.H.Daverveldt, Comp. Phys. Comm. 40(1986) 285.
- [7] For $\mu^+\mu^-$ and e^+e^- channels, MUSTRAAL is used, and KORALZ for $\tau^+\tau^-$, see for instance: R.Kleiss, Z^0 Physics at LEP 1, Event generators and software, CERN 89-08, Vol 3, 69.
- [8] TOPAZ Collaboration, I.Adachi et al., Phys. Lett. B218 (1989) 105;
VENUS Collaboration, A.Taketani et al., Phys. Lett. B234 (1990) 202;
AMY Collaboration, Y.Sakai et al., Phys. Lett. B234 (1990) 534.
- [9] JADE Collaboration, W.Bartel et al., Phys.Lett. B152(1987) 385;
CELLO Collaboration, H.-J. Behrend et al., Z. Phys. C35 (1987) 181.
- [10] ASP Collaboration, C.Hearty et al., Phys. Rev. D39 (1989) 3207.
- [11] L3 Collaboration, B.Adeva et al., Phys. Lett. B233 (1989) 530;
ALEPH Collaboration, D.Decamp et al., Phys. Lett. B236 (1990) 86;
OPAL Collaboration, M.Z.Akrawy et al., Phys. Lett. B240 (1990) 261.
- [12] ALEPH Collaboration, D.Decamp et al., Search for Neutralino Production in Z Decays, CERN-EP/90-63 (1990), Subm. to Phys. Lett. B.
- [13] J.Ellis, G.Ridolfi and F.Zwirner, Phys. Lett. B237 (1990) 423.

Table 1
Trigger and Analysis efficiencies (in %)
for the sleptons channels.

<i>Channel</i> <i>Masses (GeV/c²)</i>	$\tilde{e}^+\tilde{e}^-$ $m_{\tilde{e}} = 35$	$\tilde{\mu}^+\tilde{\mu}^-$ $m_{\tilde{\mu}} = 35$	$\tilde{\tau}^+\tilde{\tau}^-$ $m_{\tilde{\tau}} = 35$
$m_\chi = 10$	54	15	15
$m_\chi = 30$	35	14	2.6

Table 2
Trigger and Analysis efficiencies (in %)
for gauginos in two prong final states
The efficiencies include the Z^0 branching ratio into $\ell^+\ell^-$

<i>Channel</i> <i>Masses (GeV/c²)</i>	$\chi^+\chi^-$ $m_{\chi^\pm} = 40$	$\chi\chi'$ $m_{\chi'} = 40$	$\chi\chi''$ $m_{\chi''} = 80$
$m_\chi = 10$	2.8	2.2	2.7
$m_\chi = 30$	1.1	1.4	—

Table 3
Trigger and Analysis efficiencies (in %)
for gauginos in hadronic final states
The efficiencies include branching ratios

<i>Channel</i>	$\chi\chi'$	$\chi\chi'$	$\chi'\chi'$
<i>Masses (GeV/c²)</i>	$m_{\chi'} = 30$	$m_{\chi'} = 60$	$m_{\chi'} = 30$
$m_\chi = 10$	29	10	14
$m_\chi = 20$	22	13	10

Figure Captions

Fig.1. Distribution of the acoplanarity angle for the two prong events. The data are compared with the results of a Monte Carlo simulation of three standard leptonic channels using generators from ref. [5]. The triangles correspond to the $\tau^+\tau^-$ Monte Carlo simulation, the stars give the sum of e^+e^- and $\mu^+\mu^-$ Monte Carlo simulations and the squares are the data. The momentum and angular cuts are described in the text.

Fig.2. Correlation between the measured momenta in the two-prong event sample used in our search for stable particles. The two ellipses correspond to regions that would be populated by a stable charged objects with masses of 25 and 40 GeV/c^2 .

Fig.3. Mass limits for the three slepton families. The contours correspond to regions excluded at 95% CL by our analysis on acoplanar two prongs. The domain above the diagonal corresponds to a stable slepton. Mass limits given by TRISTAN[8], PETRA[9] and PEP[10] are also shown. Similar limits [11] from other LEP experiments are not shown.

Fig.4. Same as figure 3 for charginos. The smallest contour corresponds to the pure higgsino case while the biggest corresponds to the pure wino case. Similar limits [11] from other LEP experiments are not shown. The lower mass limit on stable charginos is deduced from ref.[8], the higher corresponds to our data.

Fig.5. Domain of MSSM mass parameters excluded by our gaugino search. The hatches indicate the region excluded at 95% CL by the combined analysis of charginos and neutralinos.

The thick lines define the domains excluded by our search for charginos. The dashed line indicates the domain of stable charginos which is also excluded. The thin lines define the domain excluded by our analysis on neutralinos. Fig.5a corresponds to $\tan\beta=2$ while fig.5b is for $\tan\beta=4$.

DELPHI

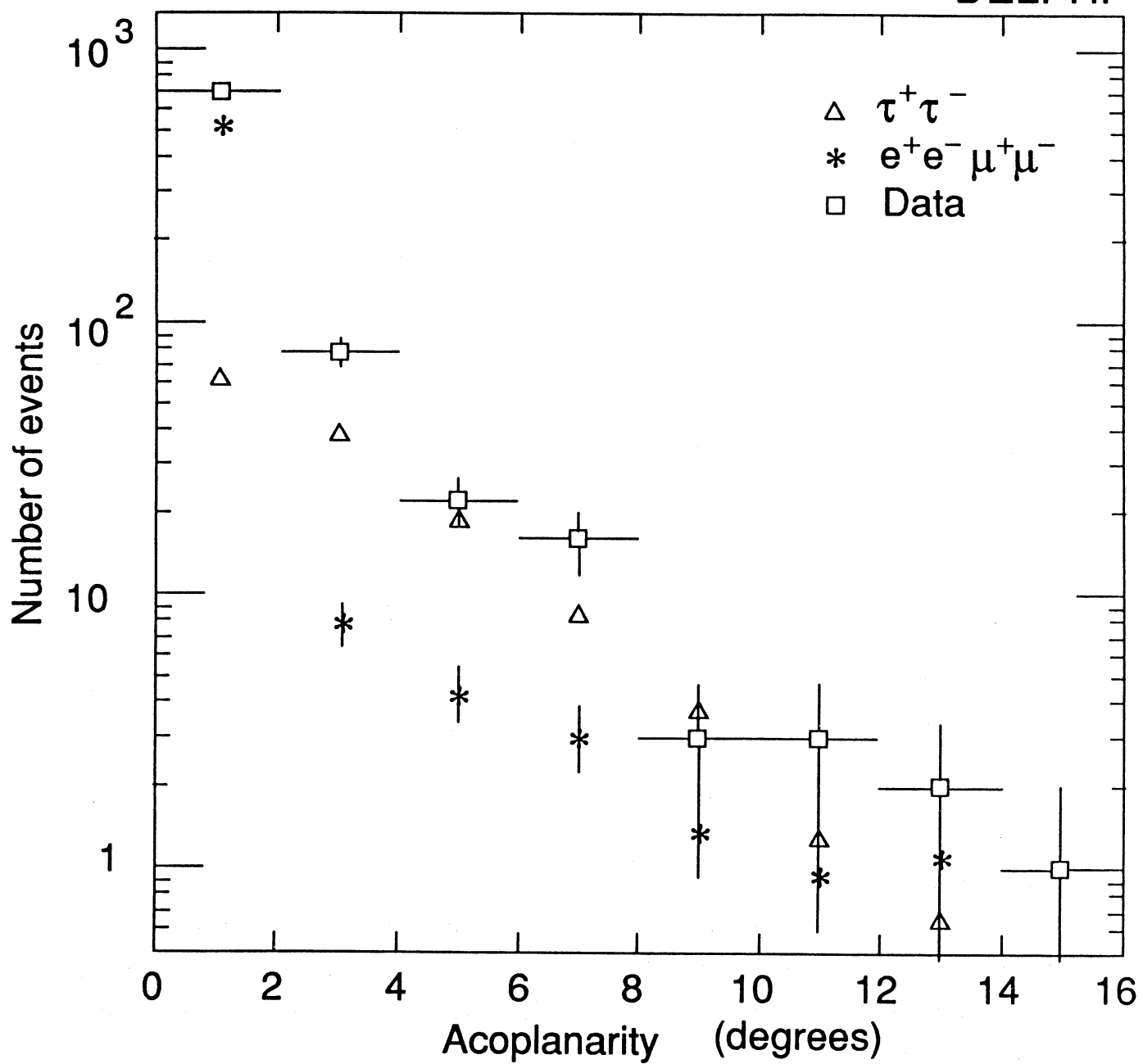


Fig. 1

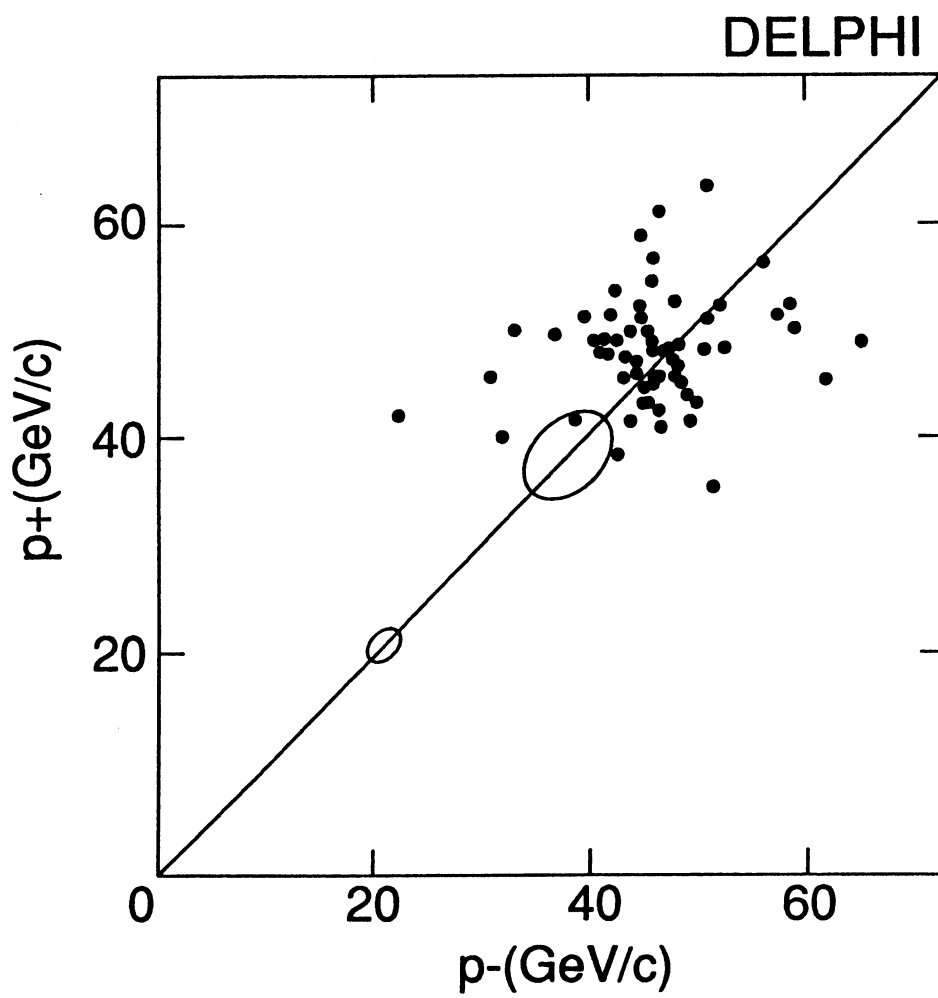


Fig. 2

DELPHI

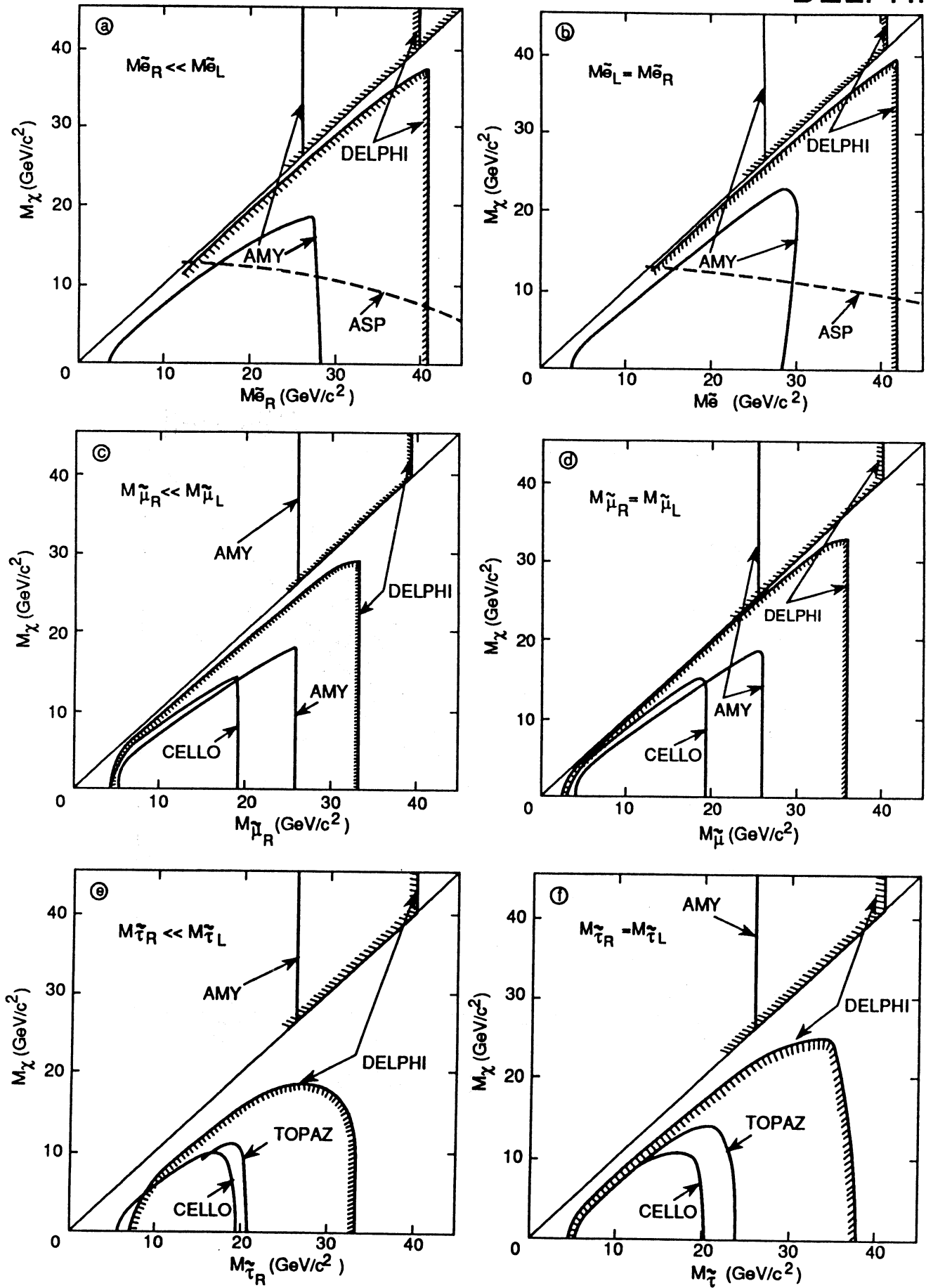


Fig. 3

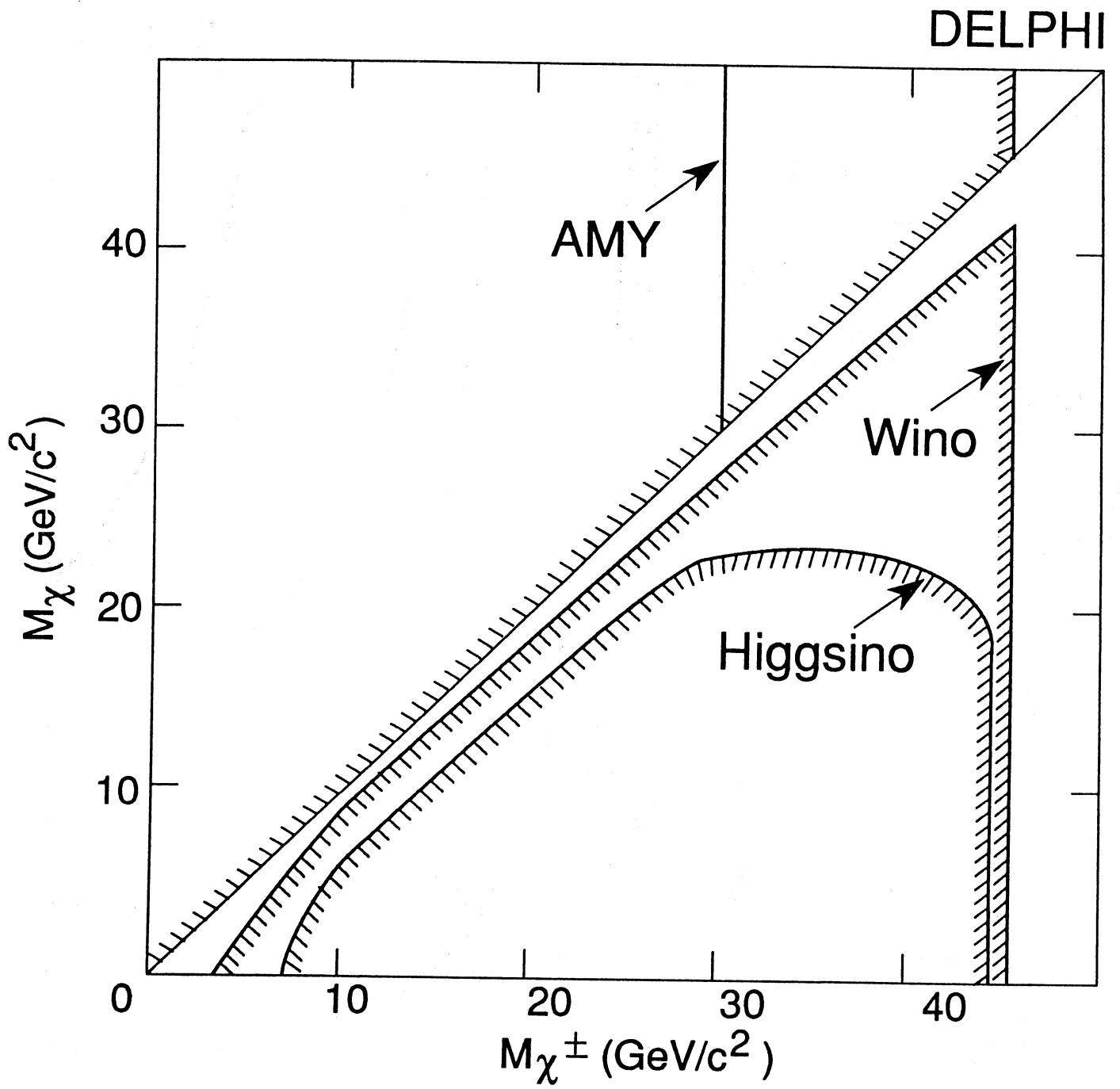


Fig. 4

DELPHI

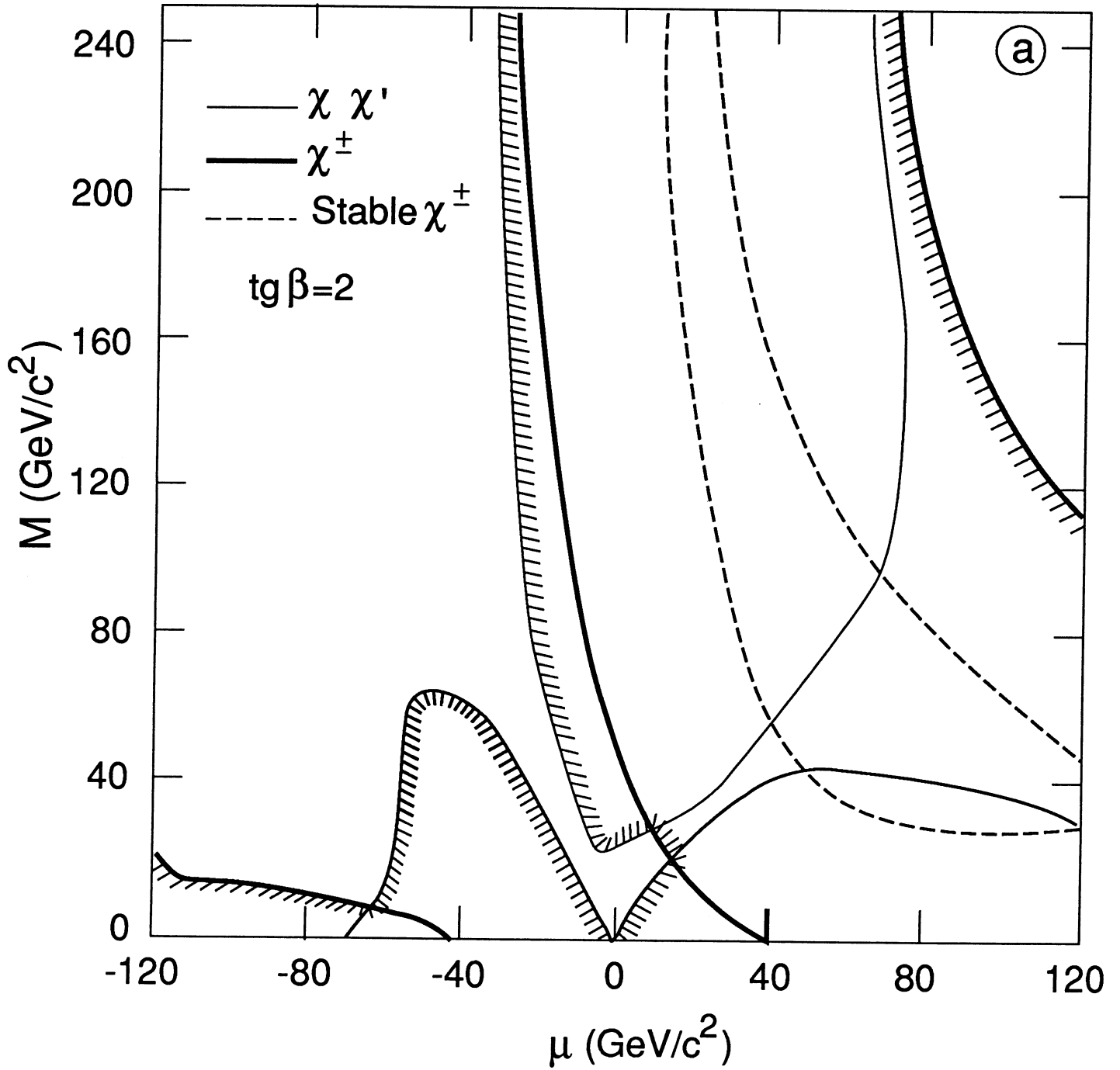


Fig.5a

DELPHI

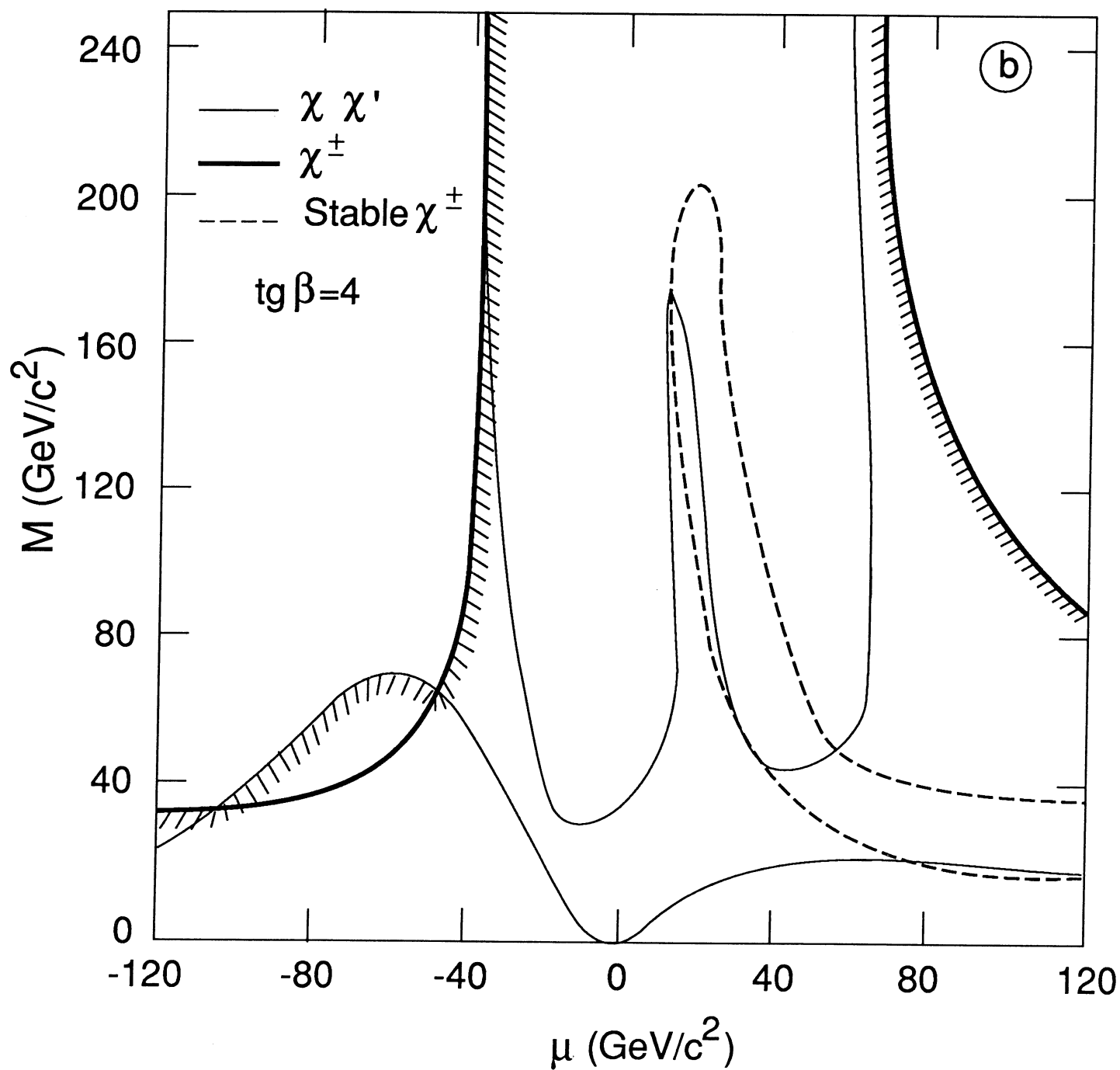


Fig.5b